Structure of Charge Density Waves in La$_{1.875}$Ba$_{0.125}$CuO$_4$

J. Sears,[1] Y. Shen,[1] M. J. Krogstad,[2,3] H. Miao,[1,4] E. Bozin,[1] I. K. Robinson,[1] G. D. Gu,[1] R. Osborn,[2] S. Rosenkranz,[2] J. M. Tranquada,[1] and M. P. M. Dean[1,*]

[1]*Department of Condensed Matter Physics and Materials Science,*
Brookhaven National Laboratory, Upton, New York 11973, USA
[2]*Materials Science Division, Argonne National Laboratory, Lemont, IL 60439, USA*
[3]*Advanced Photon Source, Argonne National Laboratory, Argonne, Illinois 60439, USA*
[4]*Material Science and Technology Division, Oak Ridge National Laboratory, Oak Ridge, Tennessee 37830, USA*
(Dated: December 16, 2022)

Although charge-density wave (CDW) correlations exist in several varieties of cuprate superconductors, they exhibit substantial variation in CDW wavevector and correlation length, indicating a key role for CDW-lattice interactions. We investigated this interaction in La$_{1.875}$Ba$_{0.125}$CuO$_4$ using single crystal x-ray diffraction to collect a large number of CDW peak intensities and refined the Cu and La/Ba atomic distortions induced by the formation of CDW order. Within the CuO$_2$ planes, the distortion involves a sinusoidal modulation of the Cu-Cu spacing along the direction of the ordering wave vector. The charge ordering within the copper-oxygen layer induces an out-of-plane breathing modulation of the surrounding lanthanum layers, which further induces a related distortion on the neighboring copper-oxygen layers. Our result implies that the induced structural distortions do not remain confined to a single layer but rather propagate a remarkably long distance through the crystal, leading to overlapping structural modulations arising from CDW distortions from different layers. We attribute this surprisingly long-range effect to the weak c-axis charge screening in cuprates.

I. INTRODUCTION

The nature of superconductivity in cuprates remains controversial; nevertheless, there is increasing evidence that charge and spin correlations might play an important role [1–4]. Experimental studies have shown that CDW correlations are ubiquitous in underdoped cuprates [5–15], while modern numerical calculations suggest that CDWs are an intrinsic feature of minimal model Hamiltonians relevant to these materials [16–19]. Cuprates such as La$_{2-x}$Ba$_x$CuO$_4$ are composed of two-dimensional CuO$_2$ layers separated by electronically inert buffer layers. Although the CDW is primarily an electronic phenomenon the rearrangements of charge associated with the CDW necessarily involves atomic displacements, which can play a substantial role in stabilizing the order. For example, measurements of phonons show a strong coupling between CDWs and the in-plane Cu-O bond stretching phonon mode [20–26]. Furthermore in La$_{2-x}$Ba$_x$CuO$_4$, the material of interest for this article, static CDW order only develops below the so-called low-temperature tetragonal (LTT) structural phase transition [5, 27–31]. Within this phase, the in-plane O atoms are displaced out of the plane (in alternating directions) along one of the Cu-O bond directions, while in the orthogonal direction the O atoms remain within the CuO$_2$ planes. This broken rotational symmetry has long been believed to pin CDW order [32], leading to a short-range CDW-structure interaction that rotates 90° from plane-to-plane due to the screw axis symmetry.

La$_{2-x}$Sr$_x$CuO$_4$, which lacks the LTT structural phase, supports a CDW order that is far weaker than that of La$_{2-x}$Ba$_x$CuO$_4$ [11, 33]. Further evidence of CDW-structure coupling is seen in the temperature-dependence of CDW-domain formation, which demonstrates that the CDW domains are pinned by the structural domain walls [34]. In this work, we use x-ray scattering to determine the atomic displacements associated with the CDW.

Modern advances in synchrotron x-ray instrumentation have made it practical to measure superlattice peaks over a large volume of reciprocal space [35]. In the present paper, we exploit these developments to collect an extensive set of diffraction data from the CDW Bragg peaks in La$_{1.875}$Ba$_{0.125}$CuO$_4$. From a fitting analysis, we are able to refine the CDW-induced displacements of the Cu and La atoms. We do not refine the O positions, due to the low sensitivity of x-rays to O atoms. We find that charge order induces a longitudinal modulation of Cu-Cu spacings within the CuO$_2$ plane. We also find that the out-of-plane La atoms show substantial displacement along the c axis, contributing to screening of the charge order. Remarkably, the modulation of the La layers leads to a similar modulation in the nearest-neighbor CuO$_2$ layer (transverse to the direction of its CDW wave vector). We attribute these long-range CDW effects to the weak c-axis charge screening in cuprates. The propagation of the distortion through the crystals helps to communicate the stripe orientation between the next-nearest-neighbor layers. Lastly, we find evidence that the CDW modulation is aligned along the direction of the tilted in-plane Cu-O bonds.

II. DATA COLLECTION

$La_{1.875}Ba_{0.125}CuO_4$ single crystal samples were grown at Brookhaven National Laboratory using the floating zone method. The samples were cut with a razor blade into pieces approximately 200 µm in all directions. X-ray diffraction data were collected at the 6-ID beamline at the Advanced Photon Source at the Argonne National Laboratory. The beam size was 500 µm and the x-ray energy was set to 87 keV to collect a large volume of reciprocal space and to minimize signal distortions due to absorption (attenuation length $\sim$ 600 µm for $La_{1.875}Ba_{0.125}CuO_4$). The samples were chosen to be smaller than the beam size and isotropic in shape in order to mitigate variation in intensity due to absorption effects or the amount of sample in the beam. We selected a sample with a mosaic spread of less than the 0.1° measurement resolution for the measurements.

The sample was cooled using a helium flow cryostat, and data were collected by continuously rotating the sample while reading out the Pilatus 2M CdTe detector every 0.1°. The images were processed by mapping each pixel into reciprocal space and then binning the pixels into a 3-dimensional grid of voxels. Bright Bragg peaks were masked on the raw images prior to binning to improve the visibility of weak features such as the CDW peaks. Two different rotations were made at different sample tilt angles, in order to fill in unpopulated voxels. The data shown correspond to a total measurement time of 4 hours.

Figure 1(a) illustrates the large extent of reciprocal space measured, and shows approximately one-sixth of the full dataset. The data were collected at 28 K, well below the simultaneous LTT structural phase transition and CDW ordering at 54 K. Throughout this work we will refer to reciprocal space positions using reciprocal lattice units (RLU), in terms of the unit cell of the high-temperature tetragonal (HTT) phase with $a = b = 3.78$ Å and $c = 13.28$ Å. We use this notation to maintain consistency with literature, even though $La_{1.875}Ba_{0.125}CuO_4$ goes through two structural transitions with decreasing temperature, entering the low-temperature orthorhombic (LTO) phase at 240 K and the low-temperature tetragonal (LTT) phase at 54 K. The unit cell of the LTO and LTT phases is larger and rotated by $\sim 45°$, leading to superlattice peaks at $(\frac{1}{2}, \frac{1}{2}, L)$ positions. These superlattice peaks are visible in the horizontal cuts of the reciprocal space shown in Fig. 1(a).

The data also show faint but clearly visible CDW signal at $\vec{q} = \pm(0.24, 0, 0.5)$ and $\vec{q} = \pm(0, 0.24, 0.5)$ positions surrounding the structural Bragg peaks, as shown in Fig. 1(b). The CDW peaks are extended and rod-like in the L direction, and are centered at half-integer L positions. These are well-known features of the CDW in $La_{1.875}Ba_{0.125}CuO_4$ – all detectable CDW peaks are of the type $(0.24, 0, 0.5)$ or $\vec{q} = \pm(0, 0.24, 0.5)$ [5, 28, 36]. The rod-like structure is due to the short correlation length in the out-of-plane direction, while the half-integer
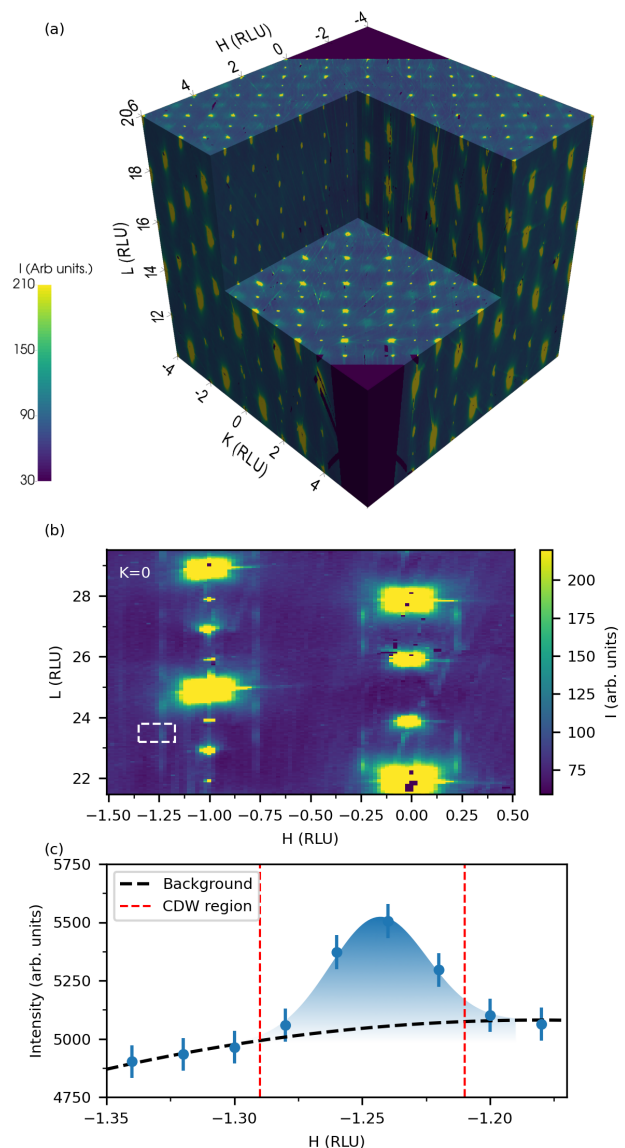

FIG. 1. $La_{1.875}Ba_{0.125}CuO_4$ CDW measurements over a large reciprocal space range. (a) Extended reciprocal space data ranging from $L = 10$ to $L = 20$, showing diffuse scattering from the high-temperature tetragonal (HTT) structure (at integer positions) and low-temperature orthorhombic (LTO)/low-temperature tetragonal (LTT) peaks at $(\frac{1}{2}, \frac{1}{2}, L)$ positions. (b) $(H0L)$ reciprocal space map showing Bragg peaks and CDW signal appearing as diffuse rods located at ± 0.24 to either side of the Bragg peaks. (c) The region indicated by the white rectangle in panel (b) summed over the K and L directions. The background was fit with a quadratic function over a small region surrounding the known peak position. Vertical red dotted lines cover 0.08 reciprocal lattice units and were chosen to encompass the CDW peak width. The points within this region were summed to give the CDW peak intensity. Error bars shown are the square root of the total photon counts. The faint streaks that form along random reciprocal space directions are detector artifacts as described in the text.
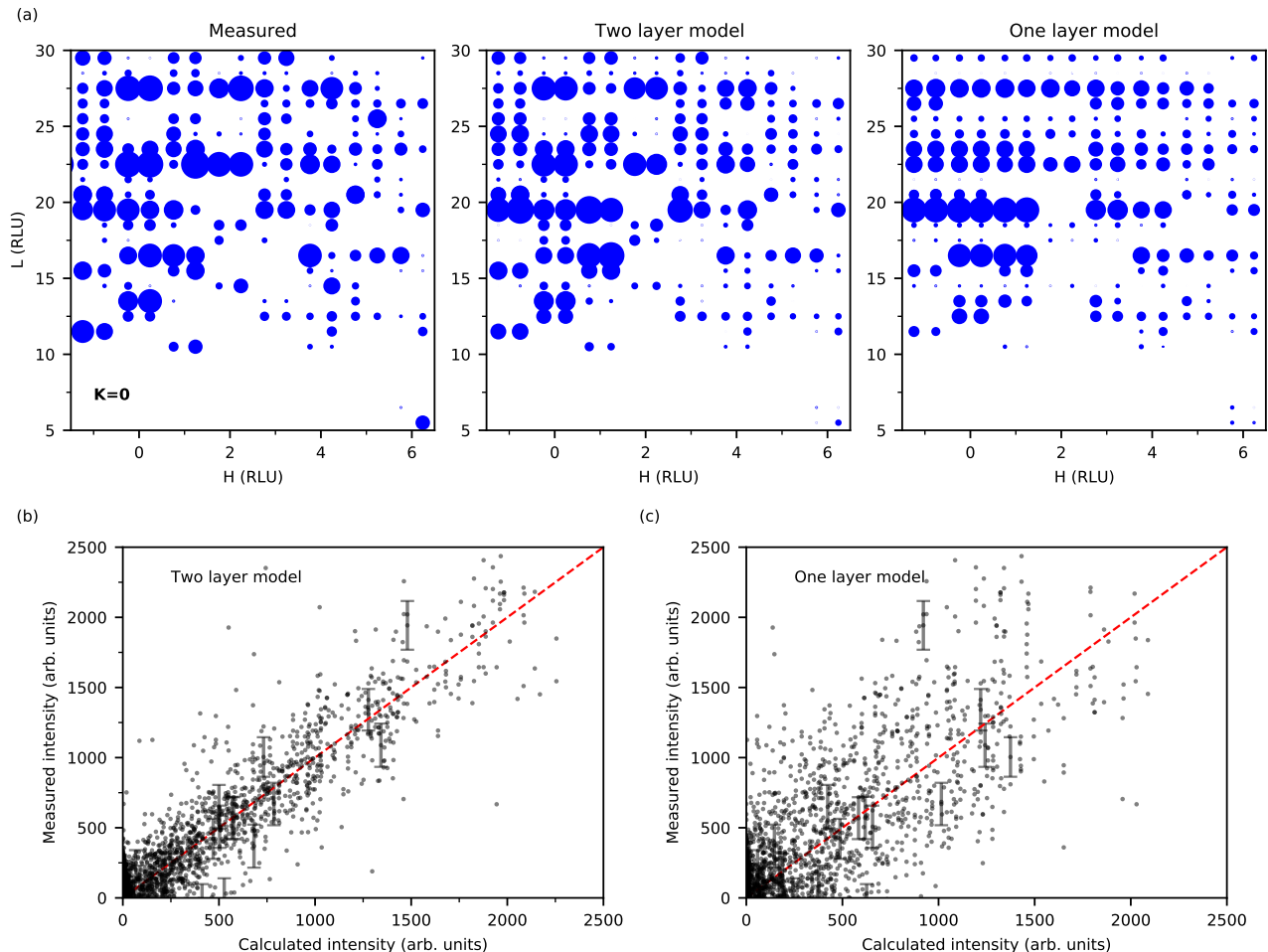
FIG. 2. Comparison of structural models with modulation of either one or both formula unit layers of the unit cell. (a) Plots of the $K = 0$ diffraction planes. Left shows the experimental data. Blank areas in the diffraction planes denote areas where a CDW intensity could not be definitely extracted. The middle and right panels shows the calculated peak intensities for the $Bbmb$ space group of irrep S1 one using modulations of either one or both planes in the crystal structure (one-layer and two-layer models respectively). In all panels, the radius is proportional to the intensity. (b) and (c) Measured vs. calculated intensity for the best fit values of the model parameters. The superior fit in panel (b) proves that the CDW induces distortions in both planes of the $La_{1.875}Ba_{0.125}CuO_4$ unit cell. For readability, the errorbars are shown for only 1% of the data points.

L peak position is a result of the out-of-phase stacking of the charge pattern between adjacent unit cells.

The intensities of the CDW peaks were extracted from this data set by summing over each peak region and subtracting the background as shown in Fig. 1(c). Despite masking of bright Bragg peaks, some streaks of intensity remain in the data due to 'blooming' from saturation of the detector. The reciprocal space map was manually inspected in the region of each peak to check for bright streaks at the CDW peak position, and contaminated peaks were excluded from the data set. The error in the peak intensity was estimated as the square root of the intensity. Due to twinning, the CDW produces peaks along both H and K. For the analysis, we chose to analyze peaks with the CDW along H i.e. peaks with $H \approx n \pm 1/4$ where n is an integer. The data were also symmetrized by reflection in the $K = 0$ mirror plane.

III. STRUCTURAL MODEL AND FITTING

While there are CDW modulations in two orthogonal in-plane directions, there is no evidence for significant coupling between these modulations. This is consistent with the CDW orientation being tied to the in-plane structural anisotropy of the LTT structure. Hence, we will analyze the modulation for just one direction, assuming that equivalent results apply for the second. The structural models were constructed assuming sinusoidal modulations of the atomic positions. The software Isodistort [37, 38] was used in our analysis to identify structures compatible with the different types of symmetry breaking that may occur in the LTT crystal structure. In our analysis, we refined our observed set of CDW Bragg peaks against a commensurate wave vector $\vec{q} = (0.25, 0, 0.5)$

from the CDW domains that lie along H, and identified four possible irreducible representations (irreps) of the parent $P4_2/ncm$ space group denoted S1, S2, S3, and S4. These irreps denote the different ways that the distortion can break the crystal symmetry, grouping together distortion modes that maintain a given symmetry operation. S1 and S3 both maintain a vertical mirror plane which is broken in S2 and S4. We will show later that the data support the preservation of the vertical mirror plane. S1 and S3 differ in the relative orientation of the CDW modulation with respect to the bent in-plane Cu-O bonds within the LTT phase. Structural refinements, which we will also outline later, support the S1 structure, which has the CDW modulation parallel to the bent in-plane Cu-O bonds. Isodistort files describing the atomic displacements involved in the different symmetry modes are provided in [39].

The individual distortion modes are sinusoidal modulations of atomic positions along the direction of the ordering vector. Phase transitions often involve only a single irreducible representation, so each of these possible distortions was refined individually against the experimental data. Each of these models includes only a subset of the free parameters required to describe the atomic positions within a suitable supercell, greatly simplifying the fitting procedure. The distortion mode model of Isodistort was converted to the crystal structure, which was used to compute the CDW peak intensities for comparison with the experimental data. The atomic form factors provided by [40] were used. The overall scale factor for the data was determined by modeling the intensity of 240 weak Bragg peaks (using the known LTT structure) and comparing with the observed intensity. A commensurate ordering vector was used for the symmetry analysis, despite the fact that the actual wave vector of the scattering is slightly incommensurate. It is thought that this shifted wave vector arises from a mixture of locally commensurate charge stripe structures [31, 41], and we will show later that the measured diffraction patterns are minimally sensitive to the phase of the CDW with respect to the underlying lattice.

We also note that since the CDW exists within the LTT structure, symmetry dictates that additional CDW peaks of the form $\vec{q} = (0.5 \pm 0.24, 0.5, 0.5)$ should exist. These are indeed present in our model, but with an intensity several orders of magnitude weaker than the $\vec{q} = (0.24, 0, 0.5)$ peaks, so it makes sense that these peaks are not detected experimentally.

The structural models of irreps S2 and S4 were found to predict very little intensity in the $K = 0$ plane. Our experimental data shows that the brightest peaks lie in this plane, and so these irreps could be immediately discarded. S1 and S3 each allow a number of possible distorted structures, and the two highest symmetry structures for each irrep were refined against the experimental data for a total of four candidate structures. For both S1 and S3, the two highest symmetry distortions had space groups $Bbmb$ and $Bmmb$.

Initial refinements of each of the candidate structures were done allowing all of the La and Cu x and z modulation amplitudes to vary. Along the reciprocal space K direction the peak intensities decrease rapidly, suggesting that the distortions in this direction are small. The y direction modulations were therefore fixed to zero. Several of the refined modulations were found to be small in comparison to their computed errors. These values were also fixed to zero, resulting in minimal models with only 6 free parameters for each of the candidate structures. Adding further parameters to these models did not substantially improve the goodness of fit. In particular, refining the modulation of the oxygen positions resulted in only minor improvements in the fit considering the large number of additional parameters added. This is not surprising considering the small contribution of oxygen to the scattering in comparison the the heavier atoms in the crystal. The oxygen distortions were therefore not included in the refinement.

IV. RESULTS AND DISCUSSION

The unit cell of $La_{2-x}Ba_xCuO_4$ contains two $La_{1.875}Ba_{0.125}CuO_4$ formula units, related at low temperature by a screw axis parallel to the crystal c axis. Each formula unit layer consists of a copper-oxygen plane and its surrounding lanthanum atoms. Throughout this discussion, we will refer to layers with the CDW ordering wave vector along the direction of the bent Cu-O-Cu bonds as 'Layer 1'. The remaining formula unit layers, with the wave vector along the straight Cu-O-Cu bonds, will be referred to as 'Layer 2'. Fig. 3 shows how the crystal structure is constructed out of alternating layers 1 and 2. These two layer types are thought to account for the two CDW domains, with the ordering vector in adjacent layers rotated by 90°, consistent with the screw axis symmetry. Our data set consists of peaks from only one of the two domains, and so we initially considered structural models in which the CDW induced distortion was confined to a single layer type. Regardless of the structural model used, allowing only a single layer to distort produced only very poor fits to the data, and failed to reproduce the qualitative features seen in the diffraction pattern as shown in Fig. 2.

Good fits to the data could only be achieved by allowing both layers to distort. When this was done, the qualitative features of the diffraction pattern could be reproduced with all four of the remaining candidate structures: space groups $Bbmb$ and $Bmmb$ for each of the S1 and S3 irreps. In all cases the χ^2 values were ~ 1, however the fits for the S3 structures were slightly worse ($\chi^2 = 1.06$ for both $Bbmb$ and $Bmmb$) in comparison with S1 ($\chi^2 = 1.02$ for both $Bbmb$ and $Bmmb$). The refined structures for S1 and S3 are very similar, the only difference being which copper-oxygen plane hosts the charge order. In the S1 structures Layer 1 hosts charge order, with the CDW ordering vector along the
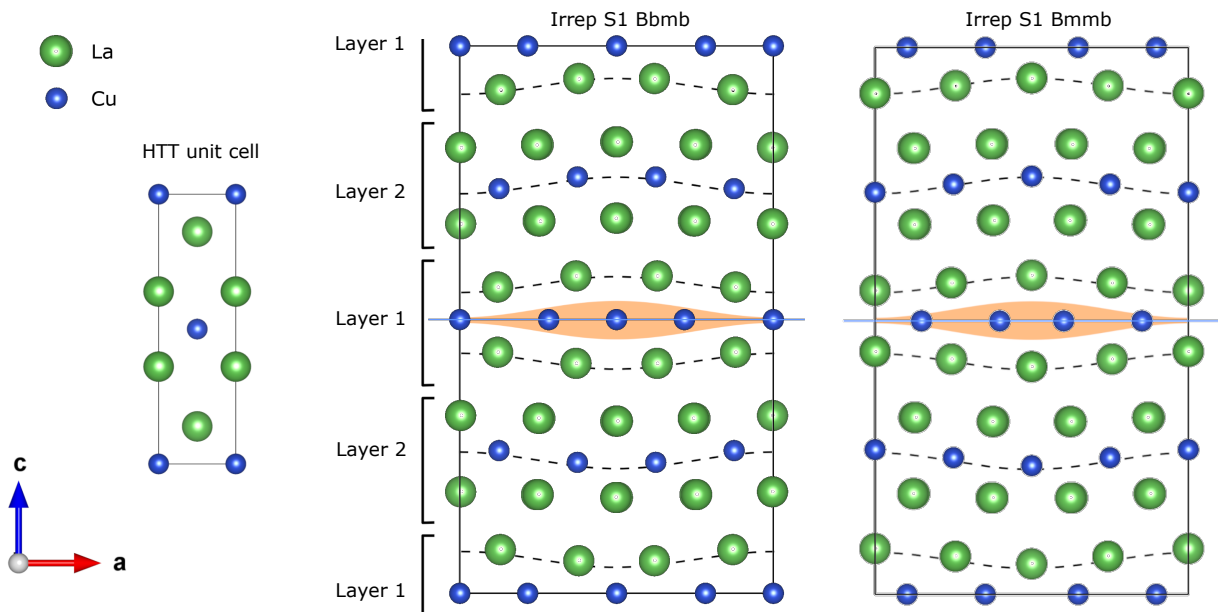
FIG. 3. The two refined structural distortions found to best fit the data corresponding to the *Bbmb* and *Bmmb* space group of the S1 irrep. These structures show the modulation of the atomic positions away from the flat planes of the HTT structure. The modulations result in a $4 \times 2 \times 2$ supercell compared with the HTT structure, as shown by the black outlines. The CDW order causes in-plane modulation of the copper positions on the central plane (blue solid line), and a breathing type distortion is transmitted to the surrounding layers of atoms (modulation shown by dashed lines). Based on the observed distortion, the probable pattern of hole density modulation is illustrated by the orange shading on the central plane. The two refined distortions are very similar, differing only in the phase of the modulation with respect to the crystal structure. The size of the distortion has been increased by a factor of 100 for visibility, and the structures were plotted using Vesta [42].

direction of the bent copper-oxygen bonds. In the S3 structures Layer 2 hosts the charge order, and the ordering vector is along the straight copper-oxygen bonds. The reason for the similarity in the fits is that the two layers have only small structural differences. Nevertheless, the slight difference in the fit quality suggests that the charge ordering vector is in the direction of the bent copper-oxygen-copper bonds. The refined structures were very similar, and from this point forward we will focus on the S1 structures.

The refined distortions are on the order of 10^{-3} Å, and are given in Table I. These values are based on the assumption that the CDW occupies 100% of the crystal. If the phase fraction is smaller, then the distortions would be rescaled accordingly. Measurements suggest that static charge order occupies the majority of the sample volume, albeit with significant disorder [43–46]. Another source of uncertainty is in the overall scaling of the CDW distortions. Due to the small CDW peak intensities, they all scale as the square of the displacements, so this scale factor cannot be independently fit with just the CDW peaks. We determined this scaling by comparing with structural Bragg peaks, which introduces possible uncertainty from self-absorption and multiple-scattering effects. Our use of a sample that is significantly smaller than the x-ray attenuation length means that this uncertainly is smaller than the uncertainty coming from do-

main population uncertainty. The relative sizes of the different distortion modes are not affected by these sources of uncertainty.

The two refined structures predict very similar diffraction patterns, with equal goodness of fit to the measured data. Figure 2(a) compares the measured diffraction pattern with the intensities predicted by the higher symmetry (space group *Bbmb*) model of the S1 irrep. This figure also shows that the best fit achieved with this model when allowing distortions in only one of the two copper-oxygen planes is quite poor. This is in contrast to the two-layer model, which is able to fit the data using only 6 free parameters to describe a data set of over 3600 peak intensities. The overall success of the fit is also demonstrated in Fig. 2(b), which shows a good match between the calculated and measured intensities for the two-layer model.

Examining the refined structures (shown in Fig. 3) shows the probable reason for the similarity in the diffraction patterns of these two candidate structures (*Bbmb* and *Bmmb* of irrep S1). The two structures are very similar, differing only in the phase of the distortion with respect to the crystal structure. Based on the equal goodness of fit, we conclude that this phase cannot be determined based on our data set. It is worth noting that fits to the data using a very similar incommensurate model gave a similarly good fit to the data. This is not unex-

pected, since the phase of the modulation with respect to the crystal is not defined in an incommensurate structure and since the *Bbmb* and *Bmmb* space groups of irrep S1, which differ in the CDW phase with respect to the underlying structure, predict very similar diffraction patterns.

Our modeling shows that the CDW in $La_{1.875}Ba_{0.125}CuO_4$ induces a longitudinal modulation of the copper atoms of one of the copper-oxygen planes (Layer 1), likely due to modulation of the hole population within this layer. The resulting charge modulation leads to a breathing-type distortion in the layers of lanthanum atoms immediately above and below this plane. The breathing distortion also propagates further into the crystal and affects nearby layers. This finding is remarkable, since the adjacent copper-oxygen layers are expected to support their own charge density wave modulations, rotated by $90°$ about the c axis. The propagation of the distortion into these adjacent layers means that in regions of the crystal where the two CDW domains coexist, the structure is described by two wave vectors rather than the simple 1D modulation usually proposed. If the modulation along the charge-stripe direction couples to the charge, then, given a $4a$ commensurability in two directions at $x = 1/8$, it might underly the remarkable doping dependence of charge order and superconductivity in $La_{2-x}Ba_xCuO_4$ [47, 48] and $La_{2-x-y}R_ySr_xCuO_4$ with R = Nd [49, 50] and Eu [6, 51].

This result can be compared with previous x-ray diffraction measurements [36], which used a structural model of distortions in a single layer to fit a far smaller data set of 70 CDW peak intensities. The authors found that the most important distortions were the longitudinal modulation of copper atoms due to the charge modula-

TABLE I. Maximum atomic displacements, with refined values for the *Bbmb* and *Bmmb* candidate structures of irrep S1. The estimated error values in parenthesis are the square root of the diagonal elements of the estimated covariance matrix, as derived from the output of the Scipy leastsq optimization function. Isodistort output files describing the distortion modes of these structures are provided as Supplemental Material [39].

Distortion Mode	*Bbmb* parameters ($Å \times 10^{-3}$)	*Bmmb* parameters ($Å \times 10^{-3}$)
A'_1(a) (Layer 2, La x)	0.19(1)	0.13(1)
A'_2(a) (Layer 2, La x)	-	-
A'_3(a) (Layer 1, La y)	-	-
A'_4(a) (Layer 2, La z)	-	-
A'_5(a) (Layer 2, La z)	0.68(1)	0.494(8)
A'_6(a) (Layer 1, La z)	1.356(6)	1.843(8)
A"(a) (Layer 1, La x)	0.33(1)	0.49(2)
Bu_1(a) (Layer 1, Cu x)	2.5(1)	1.74(8)
Bu_2(a) (Layer 2, Cu y)	-	-
Bu_3(a) (Layer 1, Cu z)	-	-
Bu_4(a) (Layer 2, Cu z)	1.42(4)	1.95(6)

tion in the copper-oxygen plane, and the modulation of lanthanum atoms along the c axis in response. Our results show that these modulations are indeed significant, but that the breathing modulation also propagates into the nearby layers.

It is also instructive to compare the distortion in $La_{1.875}Ba_{0.125}CuO_4$ to the previously solved CDW structural distortion in $YBa_2Cu_3O_{6+x}$ [52]. The first notable difference is that the copper-oxygen chain layers of $YBa_2Cu_3O_{6+x}$ are completely undistorted; in contrast $La_{1.875}Ba_{0.125}CuO_4$ hosts modulations that propagate through the crystal structure leading to modulation in all layers. The distortion of the copper-oxygen square planes also differs between the two materials. Rather than the longitudinal distortions found in the copper-oxygen planes of $La_{1.875}Ba_{0.125}CuO_4$, the distortions within the $YBa_2Cu_3O_{6+x}$ square layers are mostly along the out-of plane c direction. These results highlight the importance of the structural environment and its interaction with electronic order in the copper-oxygen planes. Of course, the zero-field CDW order in $YBa_2Cu_3O_{6+x}$ has a very short in-plane coherence length and is symmetric about a Cu-O chain layer. It would be interesting to compare with the high-field 3D CDW order in $YBa_2Cu_3O_{6+x}$ [53, 54], but this is more challenging to measure.

Since the CDW in cuprates is driven by interactions within the CuO_2 planes, our detection of CDW-induced c axis displacements of Cu and La might be considered counter-intuitive. However, the cuprates are known to have very weak electronic screening of Coulomb interactions along the c-axis. This is seen in the giant c-axis lattice constant change upon photoexcitation [55, 56] and the large oscillator strength of several c-axis-polarized phonon modes in optical conductivity and Raman measurements [57–60], including some that involve Cu and La motions [61]. Inelastic x-ray scattering measurements of $La_{1.875}Ba_{0.125}CuO_4$ also observe a substantial CDW-induced softening of c-axis longitudinal acoustic phonons [30]. Prior neutron pair distribution function measurements also associated the CDW with c-axis displacements [62]. It is further worth noting that each La^{3+} ion sits just above (or below) a square of four in-plane O^{2-} ions, so displacing La atoms involves a large modification in the c-axis Coulomb interactions. These facts make our observed long-range displacements quite natural.

V. CONCLUSIONS

Based on a comprehensive measurement of several thousand CDW peaks, we have determined the atomic displacements associated with CDW order in $La_{1.875}Ba_{0.125}CuO_4$. The structural distortion involves a sinusoidal modulation of the copper atoms along the direction of the CDW and an out-of-plane breathing modulation of the surrounding lanthanum layers. Despite the widespread belief that CDW-related distortions should rotate by $90°$ from layer-to-layer, this breathing modula-

tion, in fact, propagates further through the crystal and induces a similar distortion on the nearby copper-oxygen layers. We conclude that the effects of charge ordering cannot be considered to be confined to a single plane, but manifest as a complex long-range distortion that should be described by two wave vectors rather than the simple 1D modulation usually proposed. We attribute this surprising effect to the weak c-axis charge screening in cuprates.

[1] S. A. Kivelson, I. P. Bindloss, E. Fradkin, V. Oganesyan, J. M. Tranquada, A. Kapitulnik, and C. Howald, How to detect fluctuating stripes in the high-temperature superconductors, Rev. Mod. Phys. **75**, 1201 (2003).

[2] M. Fujita, H. Hiraka, M. Matsuda, M. Matsuura, J. M. Tranquada, S. Wakimoto, G. Xu, and K. Yamada, Progress in Neutron Scattering Studies of Spin Excitations in High-T_c Cuprates, J. Phys. Soc. Jpn. **81**, 011007 (2012).

[3] E. Fradkin, S. A. Kivelson, and J. M. Tranquada, Colloquium : Theory of intertwined orders in high temperature superconductors, Rev. Mod. Phys. **87**, 457 (2015).

[4] B. Keimer, S. A. Kivelson, M. R. Norman, S. Uchida, and J. Zaanen, From quantum matter to high-temperature superconductivity in copper oxides, Nature **518**, 179 (2015).

[5] M. Hücker, M. v. Zimmermann, G. D. Gu, Z. J. Xu, J. S. Wen, G. Xu, H. J. Kang, A. Zheludev, and J. M. Tranquada, Stripe order in superconducting $La_{2-x}Ba_xCuO_4$ $(0.095 \leq x \leq 0.155)$, Phys. Rev. B **83**, 104506 (2011).

[6] J. Fink, V. Soltwisch, J. Geck, E. Schierle, E. Weschke, and B. Büchner, Phase diagram of charge order in $La_{1.8-x}Eu_{0.2}Sr_xCuO_4$ from resonant soft x-ray diffraction, Phys. Rev. B **83**, 092503 (2011).

[7] N. K. Gupta, C. McMahon, R. Sutarto, T. Shi, R. Gong, H. I. Wei, K. M. Shen, F. He, Q. Ma, M. Dragomir, B. D. Gaulin, and D. G. Hawthorn, Vanishing nematic order beyond the pseudogap phase in overdoped cuprate superconductors, Proc. Natl. Acad. Sci. USA **118**, 10.1073/pnas.2106881118 (2021).

[8] G. Ghiringhelli, M. Le Tacon, M. Minola, S. Blanco-Canosa, C. Mazzoli, N. B. Brookes, G. M. De Luca, A. Frano, D. G. Hawthorn, F. He, T. Loew, M. M. Sala, D. C. Peets, M. Salluzzo, E. Schierle, R. Sutarto, G. A. Sawatzky, E. Weschke, B. Keimer, and L. Braicovich, Long-Range Incommensurate Charge Fluctuations in $(Y,Nd)Ba_2Cu_3O_{6+x}$, Science **337**, 821 (2012).

[9] M. Hücker, N. B. Christensen, A. T. Holmes, E. Blackburn, E. M. Forgan, R. Liang, D. A. Bonn, W. N. Hardy, O. Gutowski, M. v. Zimmermann, S. M. Hayden, and J. Chang, Competing charge, spin, and superconducting orders in underdoped $YBa_2Cu_3O_y$, Phys. Rev. B **90**, 054514 (2014).

[10] E. H. da Silva Neto, P. Aynajian, A. Frano, R. Comin, E. Schierle, E. Weschke, A. Gyenis, J. Wen, J. Schneeloch, Z. Xu, S. Ono, G. Gu, M. Le Tacon, and A. Yazdani, Ubiquitous Interplay Between Charge Ordering and High-Temperature Superconductivity in Cuprates, Science **343**, 393 (2014).

[11] V. Thampy, M. P. M. Dean, N. B. Christensen, L. Steinke, Z. Islam, M. Oda, M. Ido, N. Momono, S. B. Wilkins, and J. P. Hill, Rotated stripe order and its competition with superconductivity in $La_{1.88}Sr_{0.12}CuO_4$, Phys. Rev. B **90**, 100510 (2014).

[12] R. Comin, A. Frano, M. M. Yee, Y. Yoshida, H. Eisaki, E. Schierle, E. Weschke, R. Sutarto, F. He, A. Soumyanarayanan, Y. He, M. L. Tacon, I. S. Elfimov, J. E. Hoffman, G. A. Sawatzky, B. Keimer, and A. Damascelli, Charge Order Driven by Fermi-Arc Instability in $Bi_2Sr_{2-x}La_xCuO_{6+\delta}$, Science **343**, 390 (2014).

[13] W. Tabis, B. Yu, I. Bialo, M. Bluschke, T. Kolodziej, A. Kozlowski, E. Blackburn, K. Sen, E. M. Forgan, M. v. Zimmermann, Y. Tang, E. Weschke, B. Vignolle, M. Hepting, H. Gretarsson, R. Sutarto, F. He, M. Le Tacon, N. Barišić, G. Yu, and M. Greven, Synchrotron x-ray scattering study of charge-density-wave order in $HgBa_2CuO_{4+\delta}$, Phys. Rev. B **96**, 134510 (2017).

[14] Y. Kohsaka, C. Taylor, K. Fujita, A. Schmidt, C. Lupien, T. Hanaguri, M. Azuma, M. Takano, H. Eisaki, H. Takagi, S. Uchida, and J. C. Davis, An Intrinsic Bond-Centered Electronic Glass with Unidirectional Domains in Underdoped Cuprates, Science **315**, 1380 (2007).

[15] T. A. Webb, M. C. Boyer, Y. Yin, D. Chowdhury, Y. He, T. Kondo, T. Takeuchi, H. Ikuta, E. W. Hudson, J. E. Hoffman, and M. H. Hamidian, Density Wave Probes Cuprate Quantum Phase Transition, Phys. Rev. X **9**, 021021 (2019).

[16] B.-X. Zheng, C.-M. Chung, P. Corboz, G. Ehlers, M.-P. Qin, R. M. Noack, H. Shi, S. R. White, S. Zhang, and G. K.-L. Chan, Stripe order in the underdoped region of the two-dimensional hubbard model, Science **358**, 1155 (2017).

[17] E. W. Huang, C. B. Mendl, S. Liu, S. Johnston, H.-C. Jiang, B. Moritz, and T. P. Devereaux, Numerical evi-

dence of fluctuating stripes in the normal state of high-T_c cuprate superconductors, Science **358**, 1161 (2017).

[18] E. W. Huang, C. B. Mendl, H.-C. Jiang, B. Moritz, and T. P. Devereaux, Stripe order from the perspective of the Hubbard model, npj Quantum Mater. **3**, 22 (2018).

[19] S. Jiang, D. J. Scalapino, and S. R. White, Ground-state phase diagram of the t-t'-J model, Proc. Natl. Acad. Sci. U.S.A. **118**, e2109978118 (2021).

[20] L. Pintschovius, D. Reznik, W. Reichardt, Y. Endoh, H. Hiraka, J. M. Tranquada, H. Uchiyama, T. Masui, and S. Tajima, Oxygen phonon branches in $YBa_2Cu_3O_7$, Phys. Rev. B **69**, 214506 (2004).

[21] D. Reznik, L. Pintschovius, M. Ito, S. Iikubo, M. Sato, H. Goka, M. Fujita, K. Yamada, G. D. Gu, and J. M. Tranquada, Electron–phonon coupling reflecting dynamic charge inhomogeneity in copper-oxide superconductors, Nature **440**, 1170 (2006).

[22] T. Tejsner, A. Piovano, A. Țuțueanu, A. T. Rømer, B. O. Wells, J.-C. Grivel, M. Boehm, and L. Udby, Anomalous dispersion of longitudinal optical phonons in oxygen-doped $La_{2-x}Sr_xCuO_{4+\delta}$, Phys. Rev. B **101**, 100504 (2020).

[23] Y. Y. Peng, A. A. Husain, M. Mitrano, S. X.-L. Sun, T. A. Johnson, A. V. Zakrzewski, G. J. Mac-Dougall, A. Barbour, I. Jarrige, V. Bisogni, and P. Abbamonte, Enhanced Electron-Phonon Coupling for Charge-Density-Wave Formation in $La_{1.8-x}Eu_{0.2}Sr_xCuO_{4+\delta}$, Phys. Rev. Lett. **125**, 097002 (2020).

[24] J. Q. Lin, H. Miao, D. G. Mazzone, G. D. Gu, A. Nag, A. C. Walters, M. García-Fernández, A. Barbour, J. Pelliciari, I. Jarrige, M. Oda, K. Kurosawa, N. Momono, K.-J. Zhou, V. Bisogni, X. Liu, and M. P. M. Dean, Strongly correlated charge density wave in $La_{2-x}Sr_xCuO_4$ evidenced by doping-dependent phonon anomaly, Phys. Rev. Lett. **124**, 207005 (2020).

[25] Q. Wang, K. von Arx, M. Horio, D. J. Mukkattukavil, J. Küspert, Y. Sassa, T. Schmitt, A. Nag, S. Pyon, T. Takayama, H. Takagi, M. Garcia-Fernandez, K.-J. Zhou, and J. Chang, Charge order lock-in by electron-phonon coupling in $La_{1.675}Eu_{0.2}Sr_{0.125}CuO_4$, Sci. Adv. **7**, eabg7394 (2021).

[26] W. S. Lee, K.-J. Zhou, M. Hepting, J. Li, A. Nag, A. C. Walters, M. Garcia-Fernandez, H. C. Robarts, M. Hashimoto, H. Lu, B. Nosarzewski, D. Song, H. Eisaki, Z. X. Shen, B. Moritz, J. Zaanen, and T. P. Devereaux, Spectroscopic fingerprint of charge order melting driven by quantum fluctuations in a cuprate, Nat. Phys. **17**, 53 (2021).

[27] M. Fujita, H. Goka, K. Yamada, J. M. Tranquada, and L. P. Regnault, Stripe order, depinning, and fluctuations in $La_{1.875}Ba_{0.125}CuO_4$ and $La_{1.875}Ba_{0.075}Sr_{0.050}CuO_4$, Phys. Rev. B **70**, 104517 (2004).

[28] S. B. Wilkins, M. P. M. Dean, J. Fink, M. Hücker, J. Geck, V. Soltwisch, E. Schierle, E. Weschke, G. Gu, S. Uchida, N. Ichikawa, J. M. Tranquada, and J. P. Hill, Comparison of stripe modulations in $La_{1.875}Ba_{0.125}CuO_4$ and $La_{1.48}Nd_{0.4}Sr_{0.12}CuO_4$, Phys. Rev. B **84**, 195101 (2011).

[29] H. Miao, J. Lorenzana, G. Seibold, Y. Y. Peng, A. Amorese, F. Yakhou-Harris, K. Kummer, N. B. Brookes, R. M. Konik, V. Thampy, G. D. Gu, G. Ghiringhelli, L. Braicovich, and M. P. M. Dean, High-temperature charge density wave correlations in $La_{1.875}Ba_{0.125}CuO_4$ charge locking, Proceedings of the National Academy of Sciences **114**, 12430 (2017).

[30] H. Miao, D. Ishikawa, R. Heid, M. Le Tacon, G. Fabbris, D. Meyers, G. D. Gu, A. Q. R. Baron, and M. P. M. Dean, Incommensurate phonon anomaly and the nature of charge density waves in cuprates, Phys. Rev. X **8**, 011008 (2018).

[31] H. Miao, R. Fumagalli, M. Rossi, J. Lorenzana, G. Seibold, F. Yakhou-Harris, K. Kummer, N. B. Brookes, G. D. Gu, L. Braicovich, G. Ghiringhelli, and M. P. M. Dean, Formation of incommensurate charge density waves in cuprates, Phys. Rev. X **9**, 031042 (2019).

[32] J. M. Tranquada, B. J. Sternlieb, J. D. Axe, Y. Nakamura, and S. Uchida, Evidence for stripe correlations of spins and holes in copper oxide superconductors, Nature **375**, 561 (1995).

[33] T. P. Croft, C. Lester, M. S. Senn, A. Bombardi, and S. M. Hayden, Charge density wave fluctuations in $La_{2-x}Sr_xCuO_4$ and their competition with superconductivity, Phys. Rev. B **89**, 224513 (2014).

[34] X. M. Chen, C. Mazzoli, Y. Cao, V. Thampy, A. M. Barbour, W. Hu, M. Lu, T. A. Assefa, H. Miao, G. Fabbris, G. D. Gu, J. M. Tranquada, M. P. M. Dean, S. B. Wilkins, and I. K. Robinson, Charge density wave memory in a cuprate superconductor, Nature Communications **10**, 1435 (2019).

[35] M. J. Krogstad, S. Rosenkranz, J. M. Wozniak, G. Jennings, J. P. C. Ruff, J. T. Vaughey, and R. Osborn, Reciprocal space imaging of ionic correlations in intercalation compounds, Nat. Mater. **19**, 63 (2020).

[36] Y.-J. Kim, G. D. Gu, T. Gog, and D. Casa, X-ray scattering study of charge density waves in $La_{2-x}Ba_xCuO_4$, Phys. Rev. B **77**, 064520 (2008).

[37] H. T. Stokes, D. M. Hatch, and B. J. Campbell, Isodistort, isotropy software suite.

[38] B. J. Campbell, H. T. Stokes, D. E. Tanner, and D. M. Hatch, *ISODISPLACE*: a web-based tool for exploring structural distortions, Journal of Applied Crystallography **39**, 607 (2006).

[39] See supplemental material at [url will be inserted by publisher].

[40] D. Waasmaier and A. Kirfel, New analytical scattering-factor functions for free atoms and ions, Acta Crystallographica Section A **51**, 416 (1995).

[41] J. M. Tranquada, N. Ichikawa, and S. Uchida, Glassy nature of stripe ordering in $La_{1.6-x}Nd_{0.4}Sr_xCuO_4$, Phys. Rev. B **59**, 14712 (1999).

[42] K. Momma and F. Izumi, *VESTA3* for three-dimensional visualization of crystal, volumetric and morphology data, Journal of Applied Crystallography **44**, 1272 (2011).

[43] A. T. Savici, A. Fukaya, I. M. Gat-Malureanu, T. Ito, P. L. Russo, Y. J. Uemura, C. R. Wiebe, P. P. Kyriakou, G. J. MacDougall, M. T. Rovers, G. M. Luke, K. M. Kojima, M. Goto, S. Uchida, R. Kadono, K. Yamada, S. Tajima, T. Masui, H. Eisaki, N. Kaneko, M. Greven, and G. D. Gu, Muon spin relaxation studies of magnetic-field-induced effects in high-t[sub c] superconductors, Phys. Rev. Lett. **95**, 157001 (2005).

[44] A. W. Hunt, P. M. Singer, A. F. Cederström, and T. Imai, Glassy slowing of stripe modulation in $(La, Eu, Nd)_{2-x}(Sr, Ba)_xCuO_4$: A ^{63}Cu and ^{139}La NQR study down to 350 mK, Phys. Rev. B **64**, 134525 (2001).

[45] X. M. Chen, V. Thampy, C. Mazzoli, A. M. Barbour, H. Miao, G. D. Gu, Y. Cao, J. M. Tranquada, M. P. M. Dean, and S. B. Wilkins, Remarkable Stability of Charge

Density Wave Order in $La_{1.875}Ba_{0.125}CuO_4$, Phys. Rev. Lett. **117**, 167001 (2016).

[46] V. Thampy, X. M. Chen, Y. Cao, C. Mazzoli, A. M. Barbour, W. Hu, H. Miao, G. Fabbris, R. D. Zhong, G. D. Gu, J. M. Tranquada, I. K. Robinson, S. B. Wilkins, and M. P. M. Dean, Static charge-density-wave order in the superconducting state of $La_{2-x}Ba_xCuO_4$, Phys. Rev. B **95**, 241111 (2017).

[47] M. Hücker, M. v. Zimmermann, G. D. Gu, Z. J. Xu, J. S. Wen, G. Xu, H. J. Kang, A. Zheludev, and J. M. Tranquada, Stripe order in superconducting $La_{2-x}Ba_xCuO_4$ $(0.095 \leq x \leq 0.155)$, Phys. Rev. B **83**, 104506 (2011).

[48] A. R. Moodenbaugh, Y. Xu, M. Suenaga, T. J. Folkerts, and R. N. Shelton, Superconducting properties of $La_{2-x}Ba_xCuO_4$, Phys. Rev. B **38**, 4596 (1988).

[49] N. Ichikawa, S. Uchida, J. M. Tranquada, T. Niemöller, P. M. Gehring, S.-H. Lee, and J. R. Schneider, Local Magnetic Order vs Superconductivity in a Layered Cuprate, Phys. Rev. Lett. **85**, 1738 (2000).

[50] M. K. Crawford, R. L. Harlow, E. M. McCarron, W. E. Farneth, J. D. Axe, H. Chou, and Q. Huang, Phys. Rev. B **44**, 7749 (1991).

[51] Suryadijaya, T. Sasagawa, and H. Takagi, Oxygen isotope effect on charge/spin stripes in $La_{1.8-x}Eu_{0.2}Sr_xCuO_4$, Physica C **426–431**, 402 (2005).

[52] E. M. Forgan, E. Blackburn, A. T. Holmes, A. K. R. Briffa, J. Chang, L. Bouchenoire, S. D. Brown, R. Liang, D. Bonn, W. N. Hardy, N. B. Christensen, M. V. Zimmermann, M. Hücker, and S. M. Hayden, The microscopic structure of charge density waves in underdoped $YBa_2Cu_3O_{6.54}$ revealed by x-ray diffraction, Nature Communications **6**, 10064 (2015).

[53] S. Gerber, H. Jang, H. Nojiri, S. Matsuzawa, H. Yasumura, D. A. Bonn, R. Liang, W. N. Hardy, Z. Islam, A. Mehta, S. Song, M. Sikorski, D. Stefanescu, Y. Feng, S. A. Kivelson, T. P. Devereaux, Z.-X. Shen, C.-C. Kao, W.-S. Lee, D. Zhu, and J.-S. Lee, Three-dimensional charge density wave order in $YBa_2Cu_3O_{6.67}$ at high magnetic fields, Science **350**, 949 (2015).

[54] J. Chang, E. Blackburn, O. Ivashko, A. T. Holmes, N. B. Christensen, M. Hücker, R. Liang, D. A. Bonn, W. N. Hardy, U. Rütt, M. v. Zimmermann, E. M. Forgan, and S. M. Hayden, Magnetic field controlled charge density wave coupling in underdoped $YBa_2Cu_3O_{6+x}$, Nat. Commun. **7**, 11494 (2016).

[55] N. Gedik, D.-S. Yang, G. Logvenov, I. Bozovic, and A. H. Zewail, Nonequilibrium Phase Transitions in Cuprates Observed by Ultrafast Electron Crystallography, Science **316**, 425 (2007).

[56] Z. Radović, N. Božović, and I. Božović, Photoinduced expansion of cuprate superconductors: Evidence of strong electron-lattice coupling, Phys. Rev. B **77**, 092508 (2008).

[57] S. Uchida, K. Tamasaku, and S. Tajima, c-axis optical spectra and charge dynamics in $La_{2-x}Sr_xCuO_4$, Phys. Rev. B **53**, 14558 (1996).

[58] C. C. Homes, M. Hücker, Q. Li, Z. J. Xu, J. S. Wen, G. D. Gu, and J. M. Tranquada, Determination of the optical properties of $La_{2-x}Ba_xCuO_4$ for several dopings, including the anomalous $x = \frac{1}{8}$ phase, Phys. Rev. B **85**, 134510 (2012).

[59] S. Sugai, Phonon Raman scattering in $(La_{1-x}Sr_x)_2CuO_4$ single crystals, Phys. Rev. B **39**, 4306 (1989).

[60] A. Gozar, B. S. Dennis, T. Siegrist, Y. Horibe, G. Blumberg, S. Komiya, and Y. Ando, Inhomogeneous CuO_6 tilt distribution and charge-spin correlations in $La_{2-x-y}Nd_ySr_xCuO_4$ around the commensurate hole concentration, Phys. Rev. B **68**, 052511 (2003).

[61] R. Henn, A. Wittlin, M. Cardona, and S. Uchida, Dynamics of the c-polarized infrared-active modes in $La_{2-x}Sr_xCuO_4$, Phys. Rev. B **56**, 6295 (1997).

[62] E. S. Bozin, R. Zhong, K. R. Knox, G. Gu, J. P. Hill, J. M. Tranquada, and S. J. L. Billinge, Reconciliation of local and long-range tilt correlations in underdoped $La_{2-x}Ba_xCuO_4$ $(0 \leq x \leq 0.155)$, Phys. Rev. B **91**, 054521 (2015).